593

Fiber and Integrated Optics, Volume 11, pp. 191–219
Printed in the UK.

0146-8030/92 $10.00 + .00

Active Fibres and Optical Amplifiers

DAVID N. PAYNE

Optoelectronics Research Centre
The University
Southampton, S09 5NH
England

Introduction

The incorporation of rare-earth ions into glass fibres to form fibre lasers and amplifiers is not a recent development. In fact the first glass laser ever demonstrated [1] was flash-pumped in the form of an optical fibre, a configuration that was used to overcome the difficulties of obtaining high-quality glass in bulk form. Apart from a report [2] in 1974 of laser operation in an Nd^{3+}-doped silica multimode fibre, the idea of guided-wave glass lasers attracted little attention for the next 24 years. The idea resurfaced [3] in 1985 because both optical fibre and laser-diode technologies had advanced to a stage where low-loss, rare-earth-doped, single-mode fibres could be made and high-power semiconductor sources were available to pump them. In addition, low-cost fibre components (couplers, polarizers, filters) were available, which allowed construction of complex, all-fibre ring and Fabry-Perot resonators [4] to form a unique and powerful new fibre-laser technology. Even so, it was only the announcement in 1987 of a high-gain, erbium-doped fibre amplifier (EDFA) [5] operating in the third telecommunications wavelength-window at 1.54 μm that sparked widespread interest in rare-earth-doped fibres in the optical telecommunications community. From that moment, frenzied worldwide activity has brought numerous new fibre amplifier developments and in 1990 resulted in several commercial products appearing, a time-lag of only three years after the first research announcement.

The fibre laser, on the other hand, is only now beginning to receive widespread attention as a possible contender for a well-controlled, stable light source for telecommunications, lidar, sensors, and metrology, despite its obvious advantages of high-power pulsed operation, single-frequency capability, ease of access to the resonator, and compatibility with communications fibre. Much of the current interest stems from the unique ability of a fibre laser to generate high-purity soliton pulses of a few picoseconds in duration for potential application in the soliton-based, long-haul high-capacity communications links of the future.

The small core size of the single-mode fibre allows high pump intensities for modest ($\sim$mW) pump powers. Moreover, the intensity can be maintained over long lengths, and this leads to ultra-low lasing thresholds and permits CW diode-laser-pumped operation of three-level lasers without the usual thermal problems. In conjunction with the long fluorescent lifetime of rare-earths in glass, the high pump intensity also allows efficient, high-grain (>30 dB) operation of fibre amplifiers with good saturation properties. In

Received: June 26, 1992; accepted: August 31, 1992.
This article is reproduced, with permission, from AGARD Lecture Series No. 184.

addition, compatibility with existing fibre components is excellent, allowing all-optical circuitry to be assembled with both active and passive components. This is particularly beneficial for the fibre amplifier, where splicing of the active fibre into the telecommunication link virtually eliminates troublesome Fresnel-reflection feedback, which normally limits the gain in semiconductor laser amplifiers.

Erbium-Doped Fibre Amplifiers

The erbium-doped fibre amplifier (EDFA) is now established as the preferred amplifier for operation in the third telecommunications window at 1.54 μm. It has high polarisation-insensitive gain (>40 dB), low crosstalk between signals at different wavelengths, good saturation output power, which increases with pump power, and a noise figure close to the fundamental quantum-limit (~3 dB). The excellent noise characteristics allow hundreds of amplifiers to be incorporated along the length of a fibre telecommunication link, which can then span more than 10,000 km. Compared to the alternative of a transmission link with electronic repeaters, an all-optical link has the merit that it is transparent to the transmission code format and bit rate. It can thus be uprated by changing only the transmitter and receiver but not the repeaters.

A simplified schematic diagram of an EDFA is shown in Fig. 1, while Fig. 2 shows a more realistic optical configuration. The latter emphasizes the compatibility of fibre amplifiers with the numerous fibre components, which have been developed for telecommunications use and are now being applied to the construction and control of amplifiers. Note particularly the requirement for optical isolators at the input and output to prevent feedback from reflections or Rayleigh scattering into the amplifier, which could result in undesirable laser oscillation.

Pumping the EDFA

In order to obtain an Er^{3+} population inversion and associated signal gain, the fibre amplifier is optically pumped by a diode laser via a wavelength-division-multiplexing

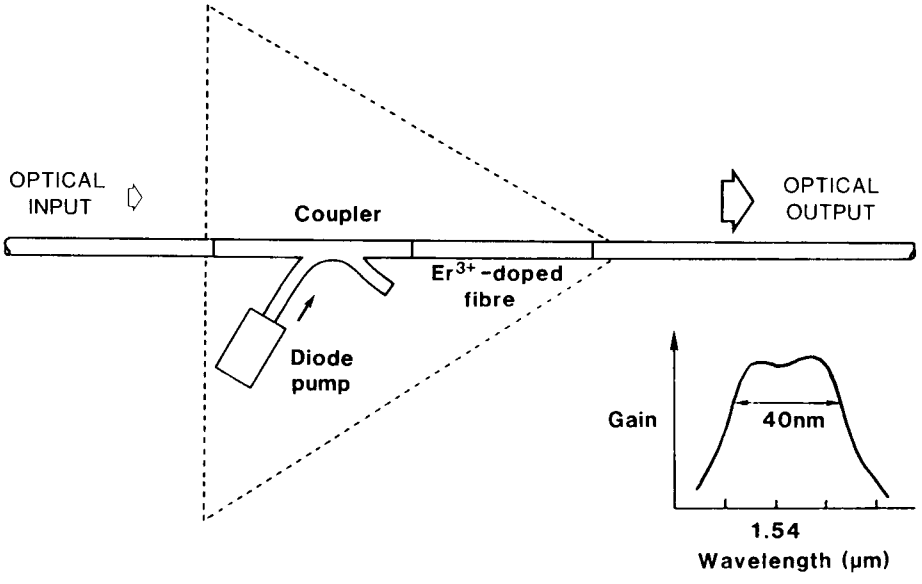

Figure 1. Schematic of erbium-doped fibre amplifier (EDFA).

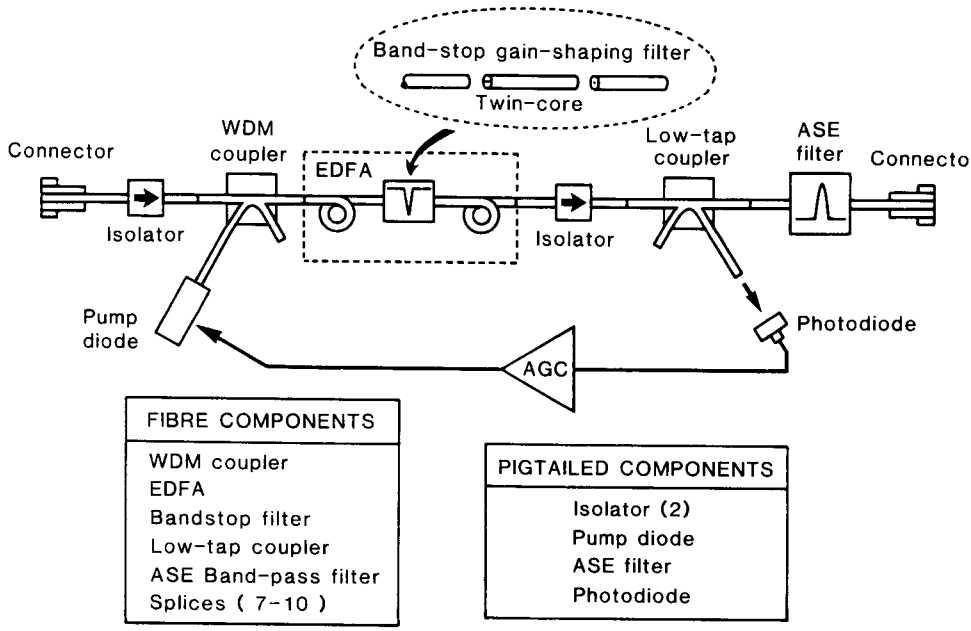

Figure 2. EDFA showing fibre components employed.

(WDM) coupler, as shown in Figs. 1 and 2. There are a number of possible pump wavelengths corresponding to the well-known Er^{3+} ground-state absorption bands (Fig. 3). Of these, potential diode-pumping wavelengths are 807 nm, 980 nm, and 1480 nm. Unfortunately, the 807 nm pump band suffers pump excited-state absorption (ESA), leading to a relatively low pump efficiency. The effect occurs when a further transition is present above the (highly populated) upper laser level with an energy difference corresponding to that of the pump photons. In this case an additional absorption (i.e., ESA) occurs at the pump wavelength, which drains pump power and limits the available gain. Nevertheless, careful choice of fibre parameters and pumping at the edge of the band (827 nm) to minimise ESA has allowed a pump efficiency of 1.3 dB/mW to be obtained [6]. For the 980 nm and 1480 nm bands, maximum pump efficiencies [7, 8] of 11 dB/mW and 5.1 dB/mW have been obtained respectively. The result for in-band pumping at 1480 nm (i.e., pumping into one of the many of the Stark components of the broad signal band) are lower than for 980 nm pumping because it is not possible to invert fully the erbium gain medium; however, a compensation for this lower efficiency is that the gain passband for 1480 nm pumping is flatter than for 980 nm pumping.

Factors that have emerged as important in achieving maximum gain for minimum pump power (max. dB/mW) are fibre numerical aperture, erbium concentration and confinement, and background loss, particularly at the pump wavelength. Unfortunately, these factors are interrelated; it is found experimentally that increasing the numerical aperture increases the fibre background loss, especially for high-erbium concentrations. The best reported result of 11 dB/mW [7] was for a fibre made by the VAD process. Results that exceed this value have yet to be reported, although fibres made in our laboratory using the MCVD fabrication process have achieved 8.9 dB/mW. Results showing gain against pump power are shown for two such fibres in Fig. 4, together with the fibre parameters. It should be recognized, however, that a trade-off exists between

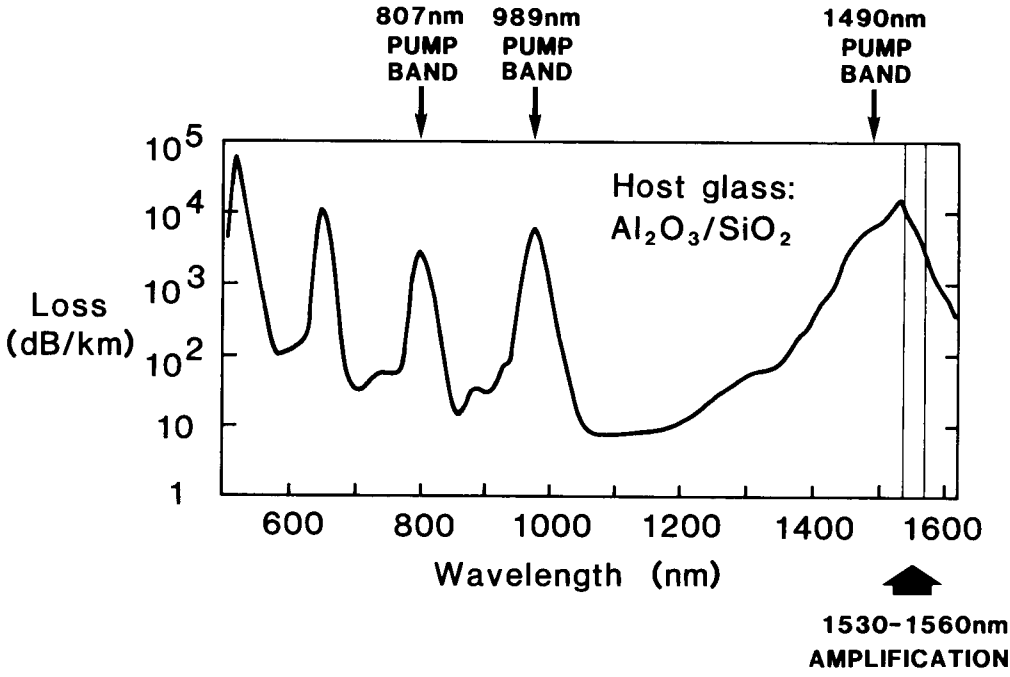

Figure 3. Pump absorption bands of Er^{3+} in $Al_2O_3SiO_2$ glass fibres.

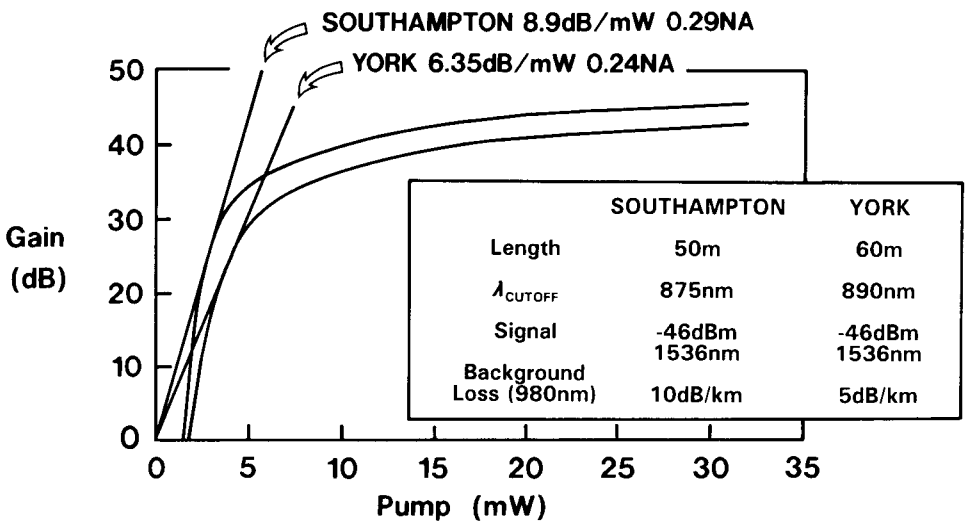

Figure 4. Gain versus pump power for two erbium-doped fibres with the characteristics shown.

gain efficiency and amplifier noise figure [9] owing to backward-travelling ASE, which saturates the input to the amplifier and reduces its gain. Just as with electronic amplifiers, reducing the gain of a low noise amplifier front-end is always detrimental to the noise performance. We calculate that amplifiers with a gain efficiency in excess of 10 dB/mW will have noise figures exceeding 4 dB.

The optimum choice of pump wavelength remains an issue to be resolved but could well depend on the intended amplifier application (i.e., as a pre-, power, or line amplifier). The 980 nm wavelength gives the best pump efficiency and noise figure, but pump diode lasers have yet to prove their long-term reliability, although it looks promising. Pump laser diodes at 1480 nm benefit from a longer development time and have proven reliability. Their electrical efficiency, however, is worse than that of 980 nm diodes, and the amplifier electrical power consumption is therefore considerably higher, especially when one takes into account the requirement for a higher optical pump power at 1480 nm because of the lower amplifier pump efficiency.

Noise

Excited states in rare-earth-doped media are subject to spontaneous as well as stimulated emission. The noise in an optical amplifier arises from the presence at the output of amplified spontaneous emission (ASE), which is given by

$$P_{\text{ASE}} = 2\mu \cdot \Delta\mu \cdot h\nu(G - 1)$$

where μ is the amplifier inversion factor, hn is the photon energy, $\Delta\nu$ is the ASE spectral width, and G is the amplifier gain. This ASE falls on the detector along with the amplified signal, whereupon the two components are mixed to give signal/spontaneous "beat" noise. The noise is so-called because the signal acts similarly to the local oscillator in a homodyne receiver and beats with the photon noise of the cw ASE power. In addition, the ASE beats with itself (spontaneous/spontaneous beat noise), and, of course, there are the usual shot noise terms associated with both signal and ASE. Assuming a detector of unit quantum efficiency, the noise power spectral density due to amplified signal and ASE is

$$\langle i^2 \rangle = \frac{2e^2}{h\nu}(A + B + C)$$

where $A = P_S + P_{SP}$ shot noise term
$B = 2\mu P_S (G - 1)$ signal/spontaneous beat term
$C = 2\Delta\nu \cdot h\nu[\mu(G - 1)]^2$ spontaneous/spontaneous beat term

where P_S and P_{SP} are the signal and spontaneous optical powers at the amplifier output. For most applications, especially if $\Delta\nu$ is made small by narrow-band filtering of the ASE at the amplifier output to match the signal bandwidth, B dominates and the noise figure is

$$\text{NF} = \frac{\text{Input signal to noise power ratio}}{\text{Output signal to noise power ratio}} = \frac{P_{\text{in}}}{P_{\text{out}}} \frac{\text{Noise}_{\text{out}}}{\text{Noise}_{\text{in}}} = \frac{1}{G^2} \frac{B}{P_S/G} \approx 2\mu$$

Thus for a fully inverted amplifier ($\mu = 1$), the NF is 2 or 3 dB.

We see that the best noise figure obtainable in an optical amplifier is quantum-

mechanically determined to be 3 dB and is limited by ASE, which mixes with the signal on a detector to produce signal/spontaneous beat noise. It can be shown that this NF translates into a best possible sensitivity of 39 photons/bit in a digital receiver, assuming a bit error rate of 10^{-9}. It should be remembered, however, that the 3 dB figure is an optimum and is dependent on the population inversion at the input to the amplifier. Although it is possible to approach a noise figure of 3 dB in the amplifier by careful attention to fibre parameters, ASE filtering, and pump power to ensure full inversion at the amplifier input, the results for a complete receiver are usually limited by the losses incurred at the input to the amplifier, which add to the noise figure. For example, the WDM coupler and isolator shown in Fig. 2 can easily add an additional 2–3 dB to the noise figure. The best reported noise figure for a complete optical pre-amplifier/receiver is 137 photons/bit, which corresponds to a noise figure of 8.6 dB [10]. Thus improvements in front-end component losses are necessary to take full advantage of the optical fibre pre-amplifier, at which point the pre-amplifier/receiver will have much the same sensitivity as the rival coherent heterodyne detection system, with less complexity.

Output Power

An important characteristic of an optical amplifier is its saturation output power. Unlike a diode amplifier, an EDFA has both a saturation output power, which increases with pump power, as well as an ability to operate deep in saturation without signal distortion and interchannel crosstalk [11]. As a consequence of these two attributes, when EDFAs are employed as power (post) amplifiers where the input signal is large and the amplifier heavily saturated, near quantum-limited differential pump-to-signal conversion efficiencies are possible [12].

When operating under deep saturation in the power amplifier mode, up to 93% quantum efficiency [12] and 77% absolute pump-to-signal conversion efficiency [13] have been respectively obtained for the two preferred pump wavelengths (980 nm and 1.48 μm). These results indicate that the amplifier is operating as a near-perfect photon convertor, and little further improvement is possible.

EDFAs capable of high output powers (>20 dBm) are needed to compensate splitting losses incurred in large-scale subscriber distribution networks and in analogue transmission of multiple TV channels. The search for EDFAs with high output power depends largely upon the availability of a sufficiently powerful and practical pump source. Approaches vary from the use of multiple-diode lasers [14] to the adoption of Nd:YAG mini-lasers [15] and Nd^{3+}-doped fibre lasers [16]. The latter two emit at a wavelength round 1.06 μm and can give output powers in excess of 1 Watt, thus showing considerable potential as pumps for EDFAs with output power approaching +30 dBm. Erbium does not possess a pump absorption band at 1.06 μm and cannot therefore normally be pumped at this wavelength. Co-doped fibres are an attractive means of alleviating constraints on the pump source wavelength by using a sensitizer with a broad absorption band. Ytterbium is especially attractive in this regard as it exhibits an intense broad absorption between 800 nm–1080 nm, spanning several convenient pump wavelength source options, including Nd^{3+}-doped fibre lasers. Figure 5 shows the pump absorption bands of Er^{3+} in silica, with the Yb^{3+} absorption superposed (cf. Fig. 3). The relevent energy levels for Er^{3+} and Yb^{3+} are shown in Fig. 6. Energy is transferred from Yb^{3+} to Er^{3+}, the efficiency of which depends strongly on the glass host. In bulk phosphate glasses this efficiency can be 85%, principally due to the reduced probability of back transfer (Er^{3+} to Yb^{3+}) for this host. We have found that SiO_2/Al_2O_3 fibres made by the

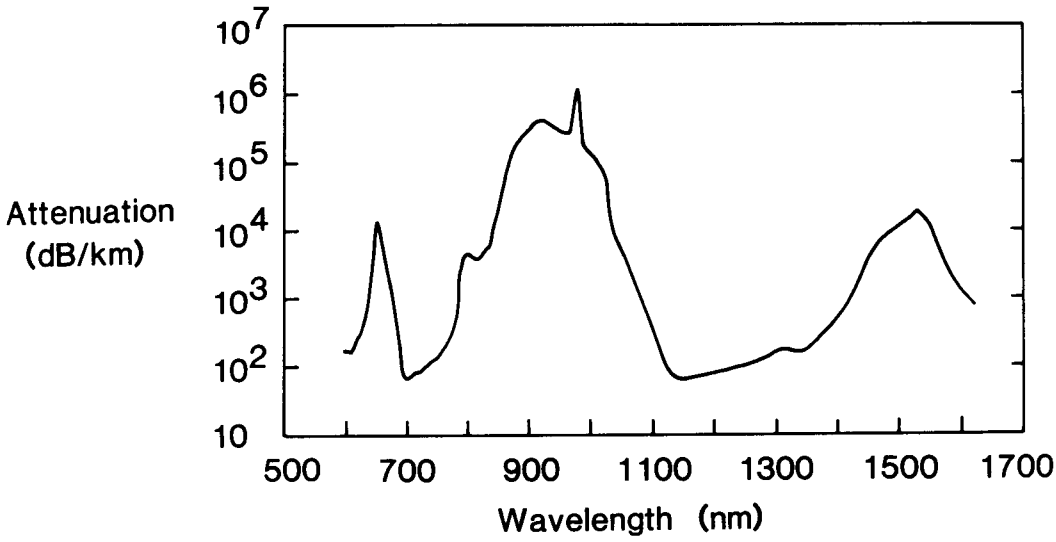

Figure 5. Absorption spectrum of Er^{3+}/Yb^{3+} co-doped fibre. Note large absorption centred at 900 nm caused by Yb^{3+}.

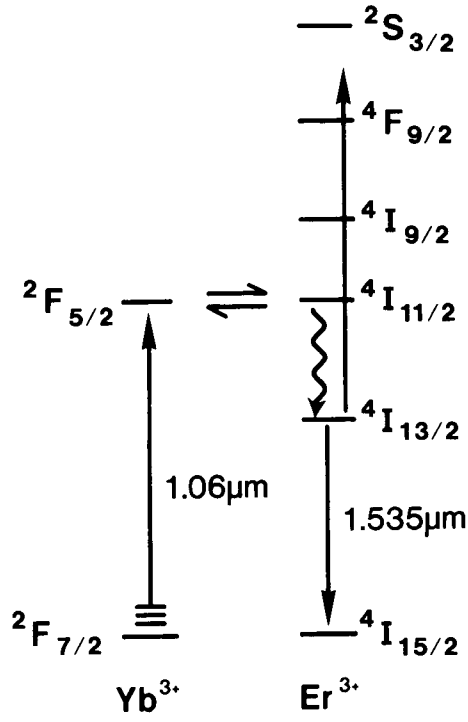

Figure 6. Er^{3+} and Yb^{3+} energy levels showing the energy-transfer pumping scheme.

MCVD process can mimic a phosphate glass provided sufficient P_2O_5 is added as a dopant. Such silica-based fibres show considerably improved transfer efficiency.

To construct a power amplifier using these fibres, a high-power, diode-pumped, Nd:YAG laser operating at 1064 nm is used to pump into the long-wavelength tail of the Yb^{3+} absorption. Such mini-YAG lasers are commercially available with output powers exceeding 1 Watt and are potentially scalable to even higher powers [17]. The Er^{3+}/Yb^{3+} fibre approach therefore shows considerable potential for EDFAs with output power approaching +30 dBm. Although not as mature as Nd:YAG mini-lasers, the cladding-pumped Nd^{3+}-doped fibre laser [16] has been shown to give an output of 1 W using a similar multi-stripe pump diode to the Nd:YAG; therefore, the fibre laser shows even greater promise as a pump source for an all-fibre, high-power EDFA.

Gain Spectrum Flattening

A number of schemes have emerged to flatten the broad (>35 mm) but unequal EDFA gain spectrum (Fig. 7) that causes problems in multichannel WDM transmission systems. Some progress can be made with choice of fibre materials, particularly Al_2O_3 co-doping and the use of ZBLAN fibres, although the most promising approach appears to be the use of an internal compensating filter within the amplifier [18]. This approach has the merit that the gain spectrum can be shaped and flattened without loss of pump efficiency and dynamic range, leading to an amplifier characterized by a gain in excess of 25 dB and a 3 dB bandwidth >30 nm for a pump power of <50 mW. The technique

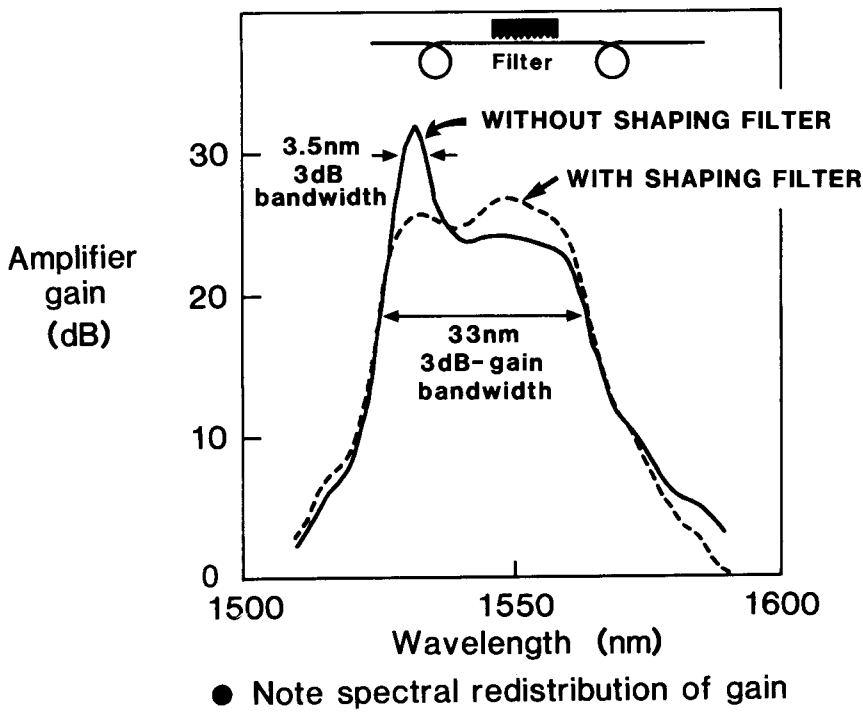

Figure 7. EDFA spectral gain profile, showing gain flattening by addition of a shaping filter within the amplifier length.

can be understood by imagining that the front half of the EDFA acts as a pre-amplifier and the remainder as a power amplifier. As is common in audio amplifiers, response-shaping is best done in the pre-amplifier, thereby preventing the power amplifier from saturating and wasting power. The spectrally shaped gain profile is shown in Fig. 7 for an amplifier with a compensating bandstop filter placed within its length in order to attenuate the gain peak, which occurs at 1536 nm. However, even with spectral shaping, for long amplifier chains involving large numbers of EDFAs, some form of spectral AGC will be required to balance precisely individual channels across a wide spectral range and prevent an accumulation of channel imbalance.

Erbium-Doped Planar-Waveguide Amplifiers

Although the planar waveguide approach to erbium-doped amplifiers is attractive, particularly for lossless splitting of a signal into a large number of output ports (Fig. 8), the search for a planar "EDFA" is plagued by erbium concentration effects, which result in a large loss of radiative quantum efficiency once the erbium concentration exceeds a few hundred ppm, an effect known as concentration quenching. This effect limits the minimum length of the amplifier to around a metre before a severe loss of efficiency occurs. Figure 8 shows the results obtained to date for the radiative quantum efficiency of Er^{3+} ions in various glass hosts, and it can be seen that a severe reduction occurs for concentrations of Er^{3+} above about 300 ppm, with fluoride glasses being the most benign host. Note that this problem is peculiar to Er^{3+} and occurs to a far smaller degree in other rare-earths, such as Nd^{3+}. The search continues to find a glass host that is able to accept a higher level of erbium doping from which amplifiers of a few cm in length can be fabricated.

Fibre Amplifiers at 1.3 μm

As can be seen from the above, the EDFA provides almost the ideal amplifier for 1.55 μm operating wavelengths. Unfortunately, 1.55 μm systems are still predominantly laboratory experiments, and although they will undoubtedly form the systems of the future, by far the largest proportion of currently operational optical transmission systems operating in the 1.3 μm wavelength window. A 1.3 μm fibre amplifier would be extremely useful for upgrading or extending existing systems. Two candidates have emerged, namely, neodymium and praseodymium-doped fibre amplifiers. In the case of neodymium-doped fibre, a transition exists between the $^4F_{3/2}$ and $^4I_{13/2}$ levels, which gives rise to fluorescence near 1.32 μm. Unfortunately, (i) a signal ESA band exists near 1.3 μm and (ii) strong competing transitions from the same level occur at 0.9 μm and 1.06 μm. The effect of the ESA is to prevent gain at wavelengths shorter than about 1.36 μm, whereas the competing transitions cause large gain to build up at other wavelengths, which must be reduced to prevent ASE losses and eventually lasing. In fluoride (ZBLAN) glass the ESA spectrum is shifted to shorter wavelengths, and 10 dB gain at 1.345 μm has been reported for only 50 mW pump power [19]. Thus to date the gain is too low and the wavelength too long for telecommunications requirements.

Perhaps the most exciting recent development has been reports of a praseodymium-doped fluoride fibre amplifier. Pr^{3+} exhibits fluorescence at 1.3 μm on the $^1G_4$- $^3H_5$ transition, but this is heavily quenched by multiphonon decay to the underlying $^3F_4$ level in all but the lowest phonon-energy glasses, hence, the choice of ZBLAN [20]. Even in ZBLAN glass, the radiative quantum efficiency has been measured at only a few per-

cent, which leads to a low amplifier pump efficiency. To compensate this, small core, high-numerical aperture fibre designs have been developed in an attempt to achieve high gains at pump powers obtainable from diode lasers. Miyajima et al. [21] demonstrated a 32 dB true amplifier gain for a pump power of 300 mW at 1.01 μm and a peak pump efficiency of 0.2 dB/mW (Fig. 9). This compares poorly with the 11 dB/mW obtained for the EDFA. However, these are early days and much effort is underway worldwide to improve the Pr^{3+}-doped fibre amplifier. The most promising approach apart from high-NA designs is to find a glass host with even lower phonon-energy than exhibited by ZBLAN to inhibit the multiphonon decay process. Several groups are working on modified fluoride glass compositions for this purpose. However, even if successful in improving pump efficiency, there are a number of engineering issues yet to be solved involving

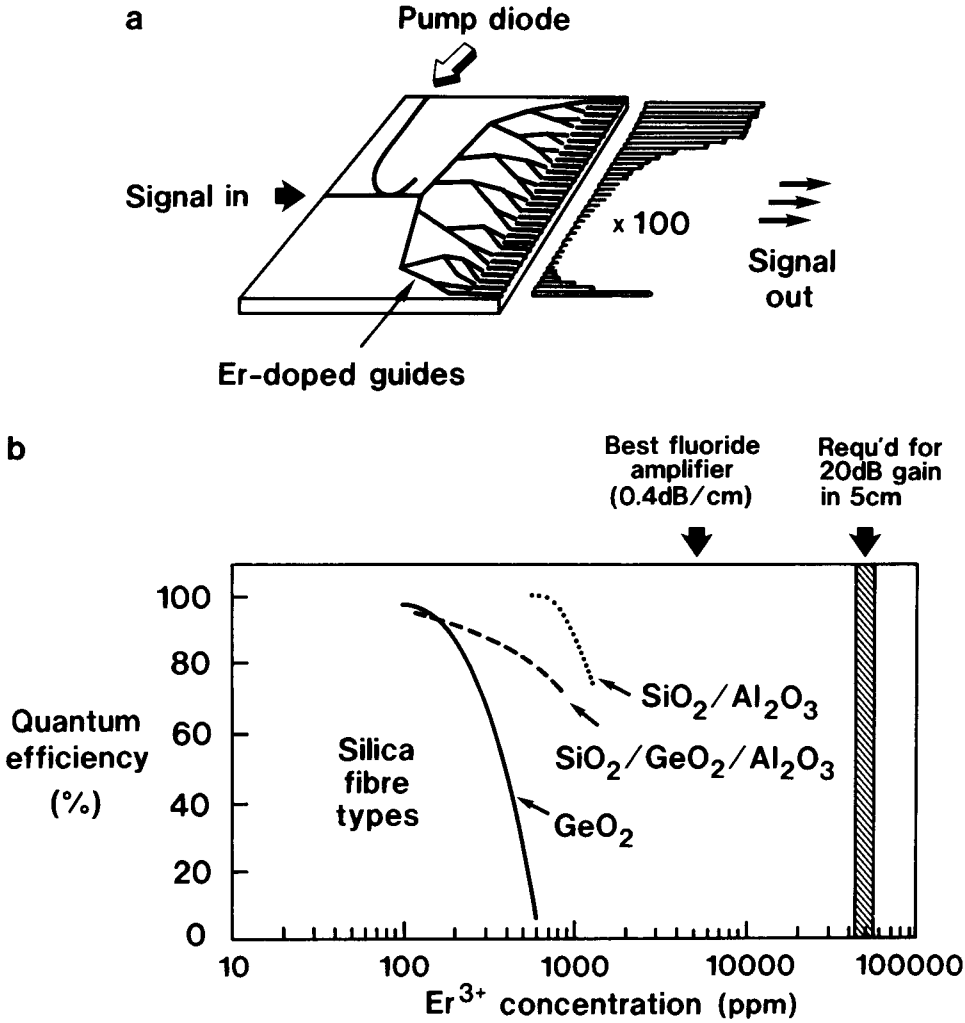

Figure 8. (a) Lossless splitting scheme in an erbium-doped planar waveguide amplifier; (b) The reduction in quantum efficiency that results from the high Er^{3+} doping required to make a short amplifier.

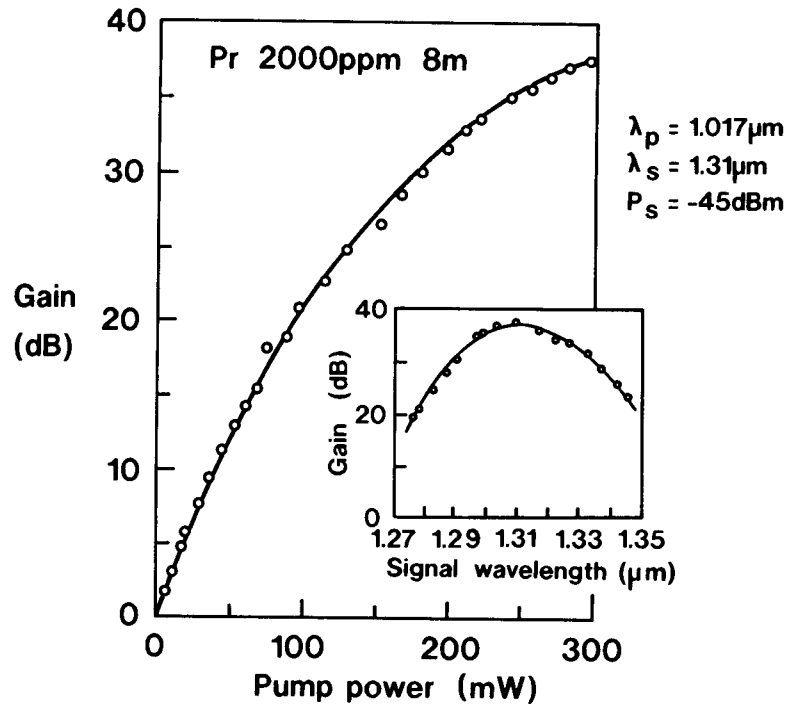

Figure 9. Gain versus pump power for a Pr^{3+}-doped ZBLAN glass fibre. Inset shows spectral gain [21].

strength, environmental stability, and splicing of ZBLAN glasses to silica communications fibre.

Systems Applications

From the foregoing it can be seen that the EDFA exhibits a performance close to that of an ideal amplifier. It is efficient, diode-pumpable, broadband, has both low noise and a high-output power and is fully compatible with fibre systems. Although undoubtedly requiring quite different amplifier designs, EDFA applications fall into three groups.

Line-Amplifiers. Line-Amplifiers replace conventional electrical repeaters in long-haul telecommunications links, particularly undersea routes. A major difference between electrical repeaters and optical amplifiers is that the optically amplified link becomes "transparent" in an electrical as well as an optical sense. The medium is no longer specific to bit-rate and format, nor even (within limits) to the wavelength of the signal, thus allowing multichannel transmission. The link is thus truly an optical conduit; a system upgrade can be achieved by changing only the terminals and not the numerous repeaters of the conventional link.

Power (Post) Amplifiers. These allow boosting of weak transmitter signals to the required power level. They also find extensive use in multiway splitting and reamplification (so-called lossless splitting). This latter application is particularly important as fibre telecommunications moves toward subscriber applications. Pump-to-signal power con-

version efficiency is clearly the prime requirement, and we have noted earlier the advances in efficient, high-power amplifiers.

Pre-Amplifiers. The third EDFA application, pre-amplifiers, allow sensitive, near quantum-limited detection in (especially) very high bit-rate systems, where electrical amplifier performance is poor. Here low noise and pump efficiency are prime requirements. Progress in these areas has also been dealt with above.

The advent of EDFA line amplifiers has raised some interesting new issues in long-haul system design. The differences between electrical and optical amplification for transmission are shown schematically in Fig. 10. Whereas long-haul transmission links were hitherto always loss-dominated, the advent of the EDFA has effectively eliminated this and virtually-lossless links of 10,000 km or more can now be contemplated. However, the one merit of electrical repeaters is that they retime and regenerate the incoming signal before retransmission and thus are able to correct any dispersion experienced by the pulses. By contrast, the optical amplifiers in a transmission link faithfully reproduce a dispersed pulse, and the designer now has to cope with up to 10,000 km (i.e., the trans-Pacific distance) of dispersion. Although adopting dispersion-shifted fibre helps considerably, it is unlikely that fibre manufacturers will be able to adjust the dispersion parameters of the fibre sufficiently accurately to ensure sufficiently low dispersion over these distances. Nonetheless, it is thought that a bit-rate of 1 Gb/sec is achievable over a distance of 10,000 km provided the dispersion in the fibre can be kept to below an average of 2.5 ps/nm.km. There is also some hope that dispersion equalization can be achieved using a compensating fibre at the end of the link having a large opposite dispersion characteristic to that of the ensemble. The bit-rate-distance projections for dispersion-shifted and non-dispersion-shifted fibre are shown in Fig. 11, which also shows that there exists a solution to the problem of dispersion, namely, the use of nonlinear transmission.

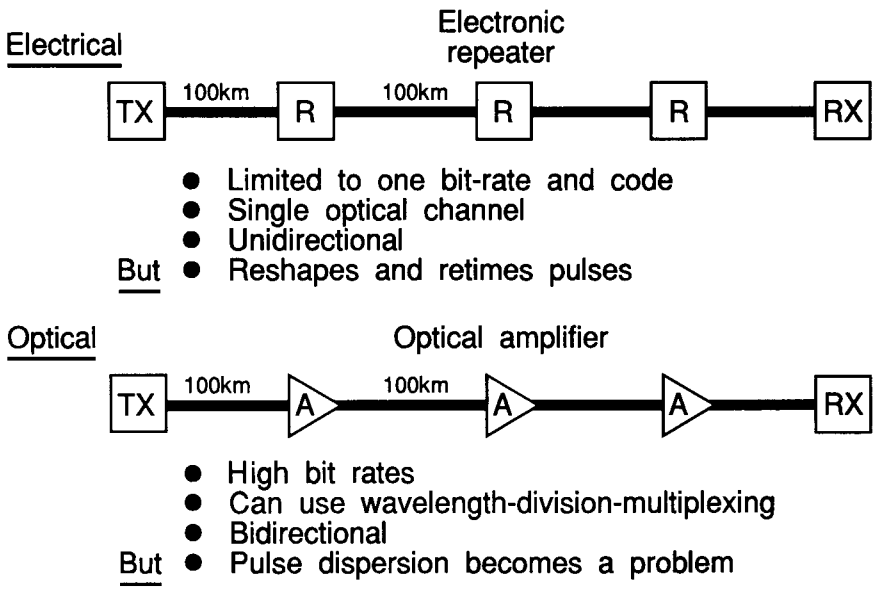

Figure 10. Comparison between electrical and optical amplification for transmission.

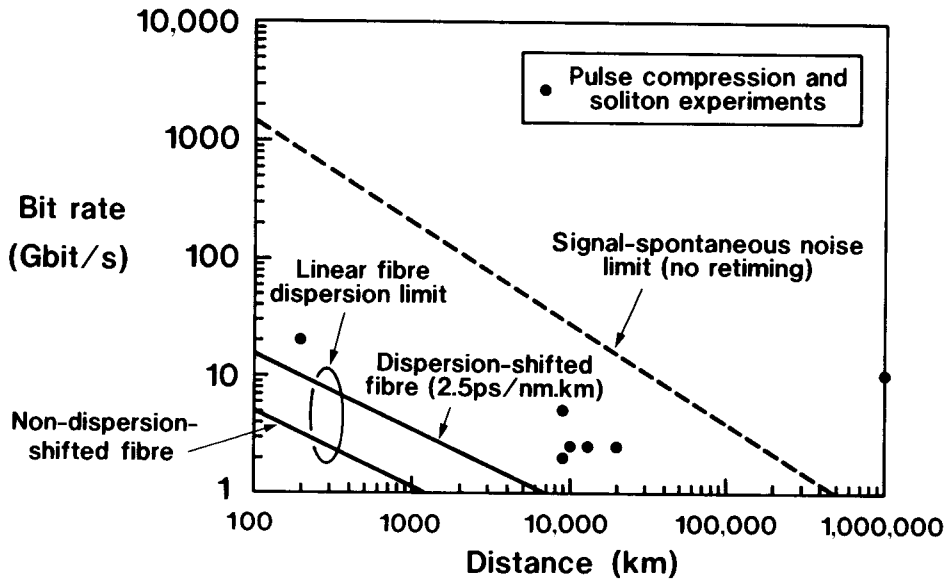

Figure 11. Bit-rate versus distance for dispersion-shifted and non-dispersion-shifted fibres. Also shown are reported nonlinear transmission experiments, together with the Gordon-Haus limit for amplified links.

Nonlinear transmission involves the use of soliton pulses. The refractive-index of glass varies slightly with optical intensity, about 10^{-13} per mW propagating in the core of a typical fibre. A consequence of this is that a pulse propagating in a glass fibre sees a moving "valley" of higher refractive-index material that travels with it. This refractive-index "valley" tends to cause bunching of high-intensity light, slowing the faster (blue) components of the pulse and speeding up the slower (red) components. It transpires that there is a critical pulse intensity and duration for which the nonlinear refractive-index change can exactly balance the natural dispersion of the fibre. Such pulses are called optical solitons and are characterized by a peak power P_s given by

$$P_s = \frac{0.0763A\lambda^3}{Cn_2} \cdot \frac{D}{\tau^2}$$

where A is the core-mode effective area, λ is the operating wavelength, D is the fibre dispersion, C is the speed of light, n_2 is the nonlinear index, and τ is the soliton FWHM duration. For a typical pulse duration of 50 ps and a fibre dispersion of 2 ps/nm.km, the peak pulse intensity required is about 1 mW, which is easily attainable using diode lasers. In theory, an optical soliton will propagate indefinitely without dispersion. Unfortunately, in practice the soliton intensity decays along the fibre owing to the fibre loss, until once below a critical intensity, the pulse suffers normal dispersion effects and rapidly broadens.

The advent of optical amplifiers has made soliton transmission a real possibility, since the soliton intensity can be boosted every 20 km or so to ensure that it does not fall below the critical dispersion threshold. Although it sounds unlikely, it transpires that the soliton pulse is a remarkably stable pulse form and proves resistant to perturbations in

fibre dispersion, multiple repeated amplification, and (to a limited extent) amplifier ASE noise. The latter effect causes a variance in pulse arrival times and provides the ultimate limit (the Gordon-Haus limit) to soliton bit-rate distance capability, shown by the dashed line in Fig. 11. Also shown in the figure are results for recent multiamplifier, soliton transmission experiments, most of which have been performed in recirculating loop configurations. From the figure it can be seen that up to two orders of magnitude improvement in distance-bit-rate product can be obtained by nonlinear transmission using solitons, and several experiments have proved the concept. Also noted in Fig. 11 is a single experimental point indicating the possibility of 10 Gbit/sec transmission over one million kilometres [22], an extraordinary result that appears to exceed the Gordon-Haus limit, an achievement that was made possible by optically reshaping the pulse periodically, as an electrical repeater.

The advent of EDFAs has made soliton transmission a reality, although there exists a variety of opinions as to whether practical telecommunications links using solitons are practical. One school of thought believes that nonlinearities in fibre will inevitably be encountered in long-haul transmission and therefore should be harnessed to advantage, while the other argues that nonlinear transmission is too complex to engineer reliably and that adequate transmission capacity can be obtained in the linear regime.

Fibre Lasers

Fibre lasers are essentially photon convertors. They use the "raw" photons emitted by diode lasers to excite rare-earth ions contained within the fibre core, which subsequently emit a stable, well-controlled laser beam. Because of the guiding properties of the fibre, the diode-laser pump light is tightly confined over the distance required for absorption, and this leads to a high population-inversion density. This large inversion density is readily obtainable in both three- and four-level laser systems at modest pump powers and gives a high single-pass gain without the usual thermal problems associated with bulk-glass lasers. The high gain, often tens of dB, allows complex resonators to be designed without undue attention to the loss of the components employed in the construction, such as couplers, isolators, and modulators. The fibre laser output is well defined, having a beam profile that is close to a diffraction-limited Gaussian. The fibre laser resonator is stable and provides a rugged, well-confined, and easily-accessed laser cavity. The diode-laser designer, on the other hand, now freed of the need to produce an optical output suitable for telecommunications, can concentrate on efficient optical power generation. This freedom of design has led to pump lasers becoming available with output powers $>$ 30 W for pumping mini-YAG lasers, and we can expect similar developments at wavelengths suitable for pumping a variety of fibre lasers.

The fibre laser geometry allows a compact, flexible layout, easy connection to optical components, and a stable, optically confined laser beam. While much of the commercial interest is likely to be in sources based on Er^{3+}, Pr^{3+}, and Nd^{3+} for optical communications, it is also important to realize that four other rare-earths have successfully been incorporated into silica hosts and operated as fibre lasers, namely, samarium, ytterbium, thulium, and holmium. An indication of the optimal pumping environment provided by the fibre laser is that laser action of Pr^{3+} and Sm^{3+} in glass has only been achieved in fibre form.

Fibre-laser oscillation covers the range 651 nm (Sm) to beyond 2 μm (Tm, Ho). Figure 12 shows the laser lines that have been reported to date, together with the loss windows of silica and fluoride-glass fibres. Erbium sits conveniently at wavelengths of

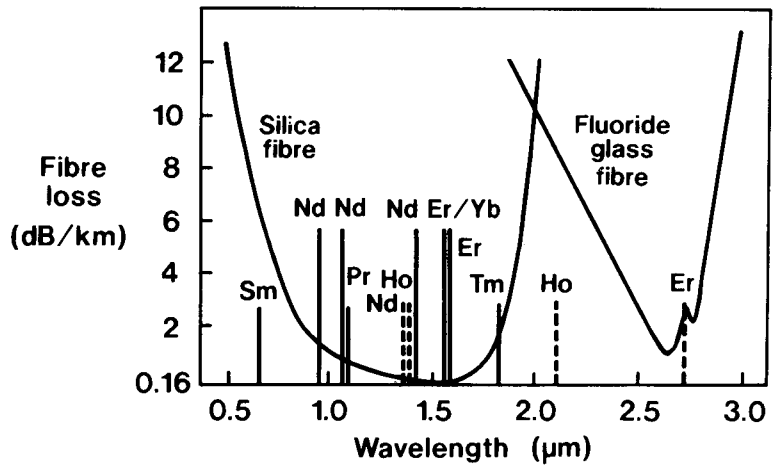

Figure 12. Reported fibre laser wavelengths compared to silica and fluoride glass fibre transmission windows.

1.54 μm and 2.7 μm, both close to the lowest loss wavelengths of these two fibre types. Furthermore, Er^{3+}-doped fibre lasers can operate with close to unity quantum efficiency [23] when pumped at 980 nm, and an output power of 5 mW is readily obtainable for launched pump powers as low as 15 mW, a power well within the range of pump diodes. A typical fibre laser Fabry-Perot resonator is shown in Fig. 13. Numerous resonator configurations are possible based on fibre-optic fused couplers, for example, ring resonators, anti-resonant-ring reflectors (fibre-loop mirrors), and Fox-Smith resonators, as well as hybrid versions of these. A useful review of fibre laser configurations is given in [24].

Current worldwide fibre-laser research covers a broad spectrum. As just one example of recent results [25], the tuning range obtained for Tm^{3+}-doped fibre lasers is shown in Fig. 14 for both an Al_2O_3-SiO_2 fibre and a GeO_2-SiO_2 fibre. The tuning range is extremely broad, being almost 300 nm (1.66 μm to 1.86 μm) for the Al_2O_3-SiO_2 host

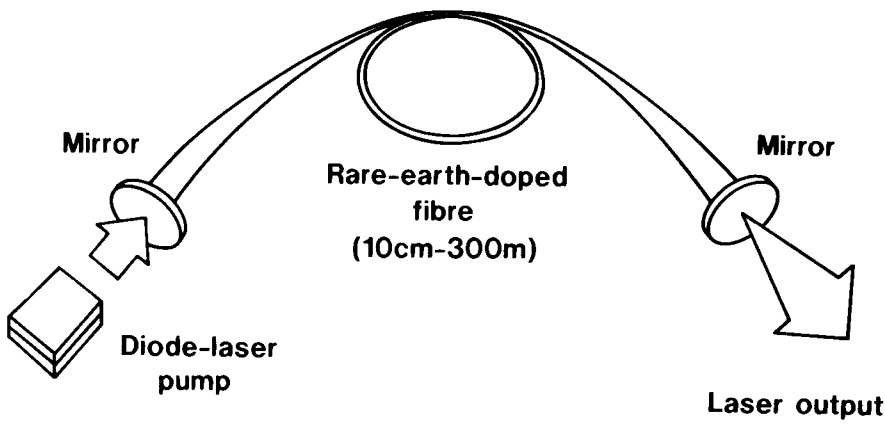

Figure 13. Fibre laser Fabry-Perot configuration.

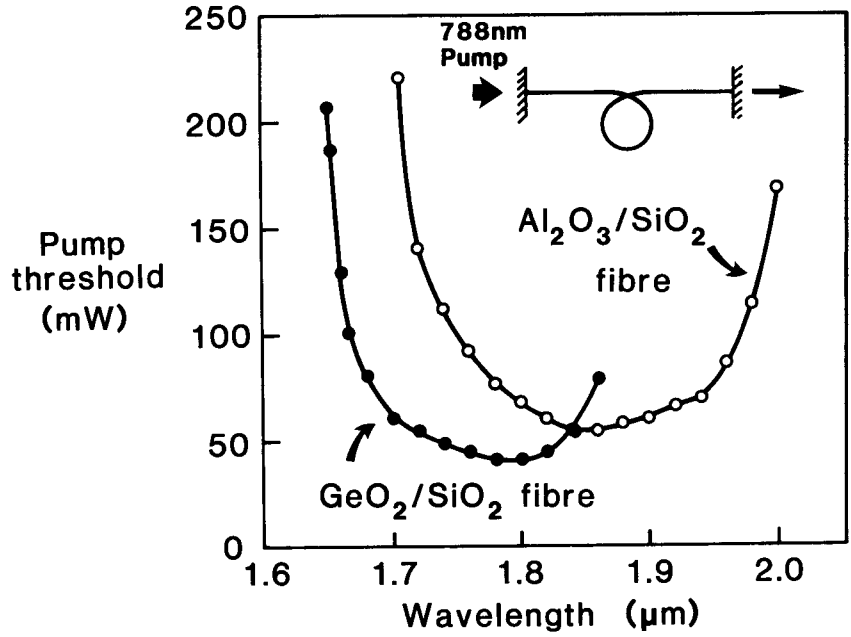

Figure 14. Tuning curves for Tm^{3+}-doped fibre lasers using either Al_2O_3 or GeO_2 as a co-dopant.

glass. Also noteworthy is the strong effect of the host glass composition (see curve for GeO_2-SiO_2 glass), a characteristic of glass-based lasers that can be usefully employed to adjust the emission wavelength of fibre lasers.

The thulium-doped fibre laser covers an extremely valuable part of the spectrum, which is eye-safe. Strong interest in this wavelength region has recently emerged for gas sensing (particularly of hydrocarbons), lidar, windshear detection, and volcanic ash cloud sensing. The wavelength can be extended to over 2 μm, and high-power lasers emitting in excess of 1 W should be possible.

High-Power Fibre Lasers

It is commonly thought that fibre lasers are low-power devices and therefore not competitive with diode-pumped bulk crystal lasers. However, by employing special glass fibre technology and novel inner-cladding geometry, it is possible to construct a Nd^{3+}-doped, single-mode fibre laser emitting an output power of 1.07 W at a wavelength of 1.057 μm. The laser is pumped with a 3 W GaAlAs multistripe, laser-diode array and has several advantages over its similarly pumped Nd:YAG counterpart. For example, the broad absorption line of Nd^{3+} in glass obviates the need for selection and temperature stabilization of the pump-diode wavelength. The waveguide nature of the fibre resonator makes mirror alignment simple, eliminates thermal focusing, and ensures perfect transverse-mode selection. The laser cavity is therefore substantially immune from environmental effects. In addition, fibre lasers are broadly tunable and, by the use of a variety of well-established fibre technique, can give high-power, Q-switched output, femtosecond mode-locked pulses, and narrow-linewidth operation. The technique of cladding-pumping [26, 27] allows pumping of single-mode fibre lasers with a multimode

diode array, thus allowing the fibre laser to exploit the increasingly available, high-power, diode-pump sources. Since the output of multistripe diode arrays is not uniphase, it cannot be efficiently launched into the core of a single-mode fibre laser. This problem is overcome by launching into the cladding of the fibre, which is designed to guide the multimode light from the diode array by the addition of a further outer cladding, as shown in Fig. 15. To optimally match the diode emission to the fibre requires careful choice of materials and design of the fibre cross-sectional geometry. The fibre utilizes compound glass technology to obtain both an optimal geometry and a high radiative cross-section. The fibre geometry is shown in Fig. 16 (inset) and comprises a heavily Nd^{3+}-doped (3 wt%) core located centrally within a rectangular, highly multimode, undoped, inner-cladding waveguide of lower-index glass into which the pump light is injected. This inner cladding was in turn clad with a further lower index glass to give a high numerical aperture (0.42) and a circular fibre cross-section. The inner cladding was thus designed to match the large diode diffraction angle and emitting area, whilst minimizing the core/inner cladding area ratio, thus optimizing pump absorption in the core and minimizing the laser threshold [28].

Pump light at 808 nm from a 3 W diode array was launched into the rectangular inner cladding of the laser fibre through a highly-reflective dichroic mirror butted to the endface; the other mirror being simply a cleaved fibre endface giving 4% Fresnel reflection. With the pump diode laser operating at full power, the fibre laser gave 1.07 W output power at a peak wavelength of 1.057 μm. As shown in Fig. 16, the slope efficiency with respect to absorbed power was around 50%, which is close to the maximum attainable.

Owing to its simplicity and robustness, the high-power fibre laser provides a competitor for diode-pumped Nd:YAG lasers in many applications, being potentially cheaper and widely tunable. Furthermore, fibre compatibility allows ready exploitation of the wide range of fibre devices available and permits integration into complex fibre optical circuits. As an example of this, the above high-power fibre laser has been used as a pump source for a high-power, Er^{3+}/Yb^{3+} fibre telecommunications amplifier at 1.54 μm, using an all-fibre tandem-pumping arrangement [29].

Tunable, Single-Frequency Fibre Lasers

One of the consequences of the very broad fluorescence linewidth of rare-earth and glass fibres is that fibre laser output emission is in general broadband, usually around 10 nm or so. Although this is of no significance in some applications, for telecommunications,

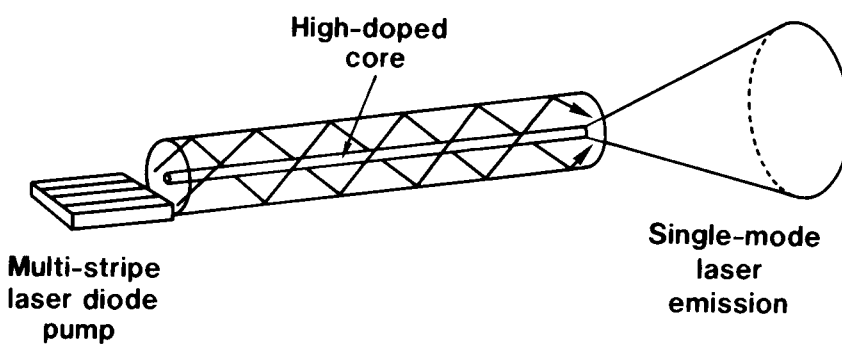

Figure 15. High-power cladding-pumped single-mode fibre laser.

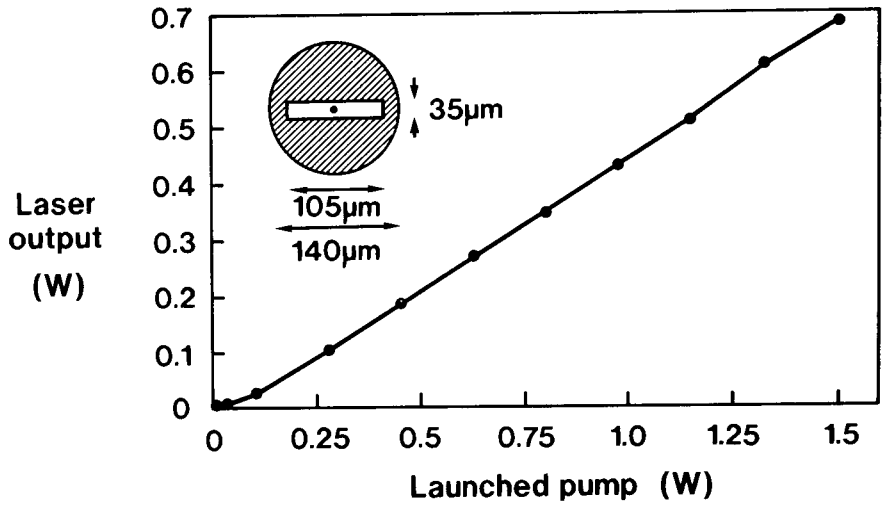

Figure 16. Nd^{3+}-doped cladding-pumped fibre laser characteristic. Inset shows fibre cross-section.

metrology or sensing the requirement is usually for only one of the numerous possible resonator modes to oscillate. This so-called "single-frequency" operation inhibits intensity noise generated by both intermode competition and mode-hopping and provides a highly monochromatic output with very low relative intensity noise. The spectral linewidth for single-frequency operation is that of just one of the resonator modes and is given by the Schawlow-Townes limit, which indicates, amongst other factors, that the linewidth is inversely proportional to the resonator length. Since typical fibre lasers are metres in length, whereas diode-lasers are submillimetre, fibre lasers can exhibit single-frequency operation with linewidths in the kilohertz region, whereas diode lasers have megahertz linewidths. This is a very attractive attribute of fibre lasers.

A less helpful consequence of the long fibre laser resonator is the close frequency spacing Δf of the axial laser modes, given by

$$\Delta f = \frac{c}{2Ln}$$

where c is the speed of light, L is the resonator (fibre) length, and n is the core refractive index. Obtaining single-frequency operation requires the selection of just one of these dense comb of oscillating laser lines. Two approaches can be taken:

1. The use of a short Fabry-Perot resonator to space the axial modes as widely as possible, in conjunction with a very narrowband Bragg reflector as one of the laser feedback mirrors [30].
2. The adoption of a travelling-wave resonator [31], which automatically encourages single-axial-mode operation by elimination of spatial hole-burning. Spatial hole-burning occurs only in standing-wave resonators and, as the name implies, "burns" out the population inversion periodically along the gain medium, thus leaving some gain unused. It transpires that the immediately adjacent axial mode to that causing the spatial hole-burning then sees higher available gain and will

oscillate, since it can effectively fill in the spatial gaps left by the first oscillating mode. It is this spatial hole-burning that encourages the laser to operate in multiple axial modes rather than just one, and its elimination immediately disposes the laser toward singe-frequency operation.

Both of the above approaches require narrowband optical filters, which ideally are fibre-based. Because the Fabry-Perot resonator approach has a standing optical wave in the resonator, the requirements for the frequency-selective component are more stringent, since the natural tendency of the laser must be overcome. On the other hand, the travelling-wave approach exploits the predisposition of the laser to operate in single-axial mode, and the frequency-selective component is used largely as a tuning element. Three main narrowband filter types have emerged with quite different characteristics, and each has been used to produce single-frequency fibre lasers. These are the fibre-relief grating [32], photorefractive Bragg-grating [33], and the miniature fibre Fabry-Perot (FFP) [34]. The fibre-relief grating applies a physical corrugation on the side of the fibre and is made by removing the fibre cladding by polishing to obtain access to the core evanescent field or by employing a D-section fibre. Photoresist is then applied and exposed holographically using a short-wavelength laser. A grating is subsequently etched into the fibre using either a dry or wet process. An index-layer is then normally applied to "lift" the field and optimize its interaction with the grating corrugations. Fibre-relief gratings act as a narrowband Bragg-reflector, and reflectivities as high as 95% with a bandwidth between 25–1800 GHz have been reported [35]. Excess losses are low (<0.5 dB), and limited tunability (3 nm) can be obtained by temperature-tuning or changing the index of the grating overlay.

An exciting recent development in narrowband filters is the technique of directly writing photorefractive-Bragg gratings within the core of a single-mode fibre [33]. An interference pattern of ultra-violet light at around 240 nm is focused onto the core of a germanium-doped silica fibre. After exposure of a few minutes, a distributed-Bragg reflector is created at a wavelength corresponding to the periodicity of the interference pattern. Using this transverse holographic technique, photorefractive gratings can be written at any wavelength and can have reflectivities up to 98%. The origin of the effect is the subject of much controversy with several theories available. There appears to be agreement that it is associated with Ge E' centres within the core, which absorb strongly at 240 nm. Fortunately, writing the gratings is accompanied by an increase in absorption of only 0.2% at 1.55 μm. Reflection linewidths of 20–100 GHz are obtainable, and the filters exhibit limited tunability (2 nm) using either temperature or strain [36]. The main appeal of photorefractive grating filters is the ease with which they can be made, their very low loss, and the noninvasive nature of the fabrication process.

Fibre Fabry-Perot filters [37] have been around for a number of years but have recently come to prominence with the development of widely tunable commercial devices. Several configurations are possible, the most popular being to deposit highly reflective multilayer dielectric mirrors on the ends of a short (<2 nm) stub fibre, which is then glue-spliced between fibre pigtails. Tuning is achieved by piezo-electrically stretching the short fibre length, which incorporates a gap for this purpose. The inclusion of a fibre waveguide within the Fabry-Perot resonator is crucial, since it prevents beam walkoff and allows a high finesse (>100) to be achieved in a compact, robust device.

Fabry-Perot filters differ from grating filters (either relief or photorefractive) in that they have a bandpass characteristic, reflecting the stopped light. In common with all

Fabry-Perot etalons, they exhibit multiple passbands, with typical bandwidths of 1–100 GHz and a free spectral range (FSR) of 100–100,000 GHz. Excess losses are <3 dB, and tunability over one or more FSR is possible.

Two examples of travelling-wave, single-frequency fibre lasers are shown in Fig. 17 and 18—one using the photorefractive Bragg-reflector or fibre-relief grating and the other using a fibre Fabry-Perot filter. Travelling-wave operation of the resonators is ensured by incorporating an isolator to prevent counterpropagating resonances. In both cases spectral linewidths of <20 kHz are achieved with very low amplitude noise and a tunability over 40 nm. These attributes makes this type of laser a very strong contender for telecommunications WDM sources. Compared with DFB diode lasers they have narrower linewidth, lower noise, and a higher output power. However, an as-yet unsolved problem is that of mode-hopping from axial mode to axial mode, which occurs when the filter precisely straddles two laser resonator modes.

It remains to be seen whether the single-frequency fibre laser will rival DFB diode lasers as the preferred narrow-linewidth telecommunications source, particularly in areas that require highly stable, narrow-band tuning capability, such as in dense WDM systems.

Mode-Locked Fibre Lasers

As with conventional lasers, fibre lasers can be Q-switched or mode-locked to produce short, high-power pulses. An advantage of the fibre configuration is that the peak-power handling capability (set by the material damage) is tens of kilowatts, a figure which considerably exceeds that obtainable from diode lasers. Thus fibre lasers can be used to convert the low-level light from a diode-laser pump into the short, high-power pulses

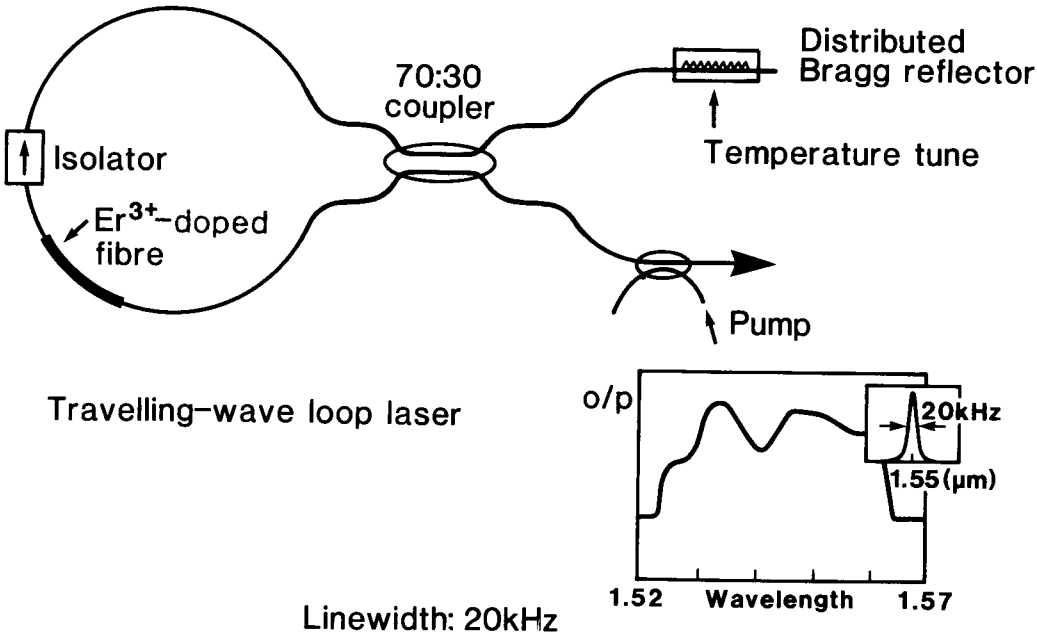

Figure 17. Tunable single-frequency loop laser using a Bragg grating as a tuning element.

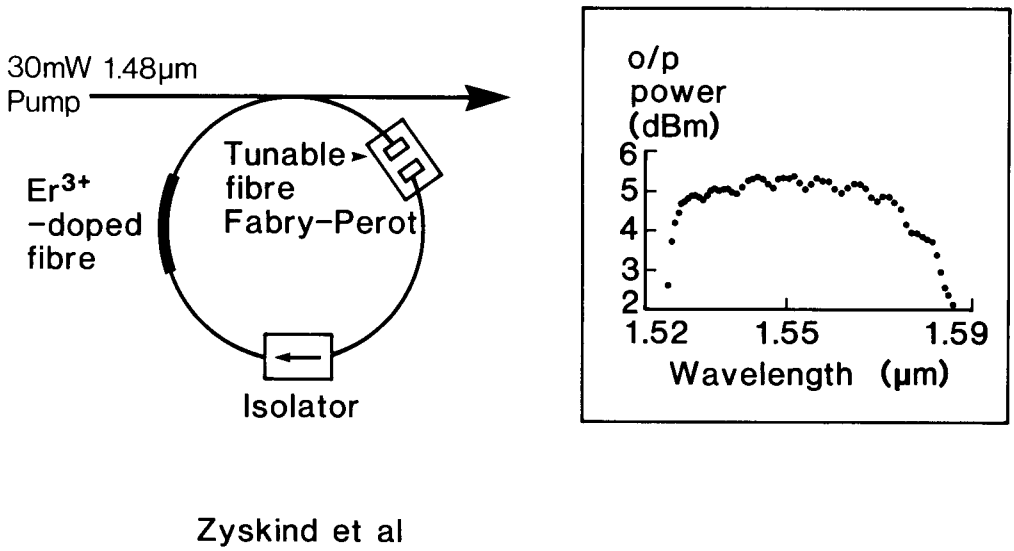

Figure 18. Tunable single-frequency travelling-wave ring laser using a fibre Fabry-Perot tuning element.

required for lidar, nonlinear switching and ranging. A few milliwatts of average output power from a fibre laser can have peak powers of many kilowatts in a pulse train.

Numerous publications have emerged which describe mode-locking and Q-switching of fibre lasers by conventional laser techniques, such as phase, amplitude, or intracavity modulation [38].

At the power levels obtainable from mode-locked fibre lasers, especially if subsequently amplified, nonlinear effects in fibres are easily accessable. Moreover, with the plethora of fibre components now available, it is relatively easy to assemble complex fibre circuits to include fibre lasers and amplifiers. Recently, this has led to a number of fibre laser/amplifier configurations emerging, which combine nonlinear switching, soliton propagation, and mode-locking. It is our purpose here to examine just one of these as illustrative of the advantages to be gained by combining nonlinear and amplifying effects.

Fibre Switches

Much work had been done to develop all-optical switches compatible with optical fibre technology. The physical mechanisms employed have been based on third-order, nonlinear effects such as Self-Phase and Cross-Phase Modulation (SPM and CPM respectively), which have response times of the order of a few femtoseconds. This ultrafast response time is tantalizing for switching and routing in ultra-high bit-rate telecommunications schemes, high-speed optical processing, and in the generation of ultra-short pulses. We will first describe the operation of an all-fibre, ultrafast switch, the Nonlinear Amplifing Loop Mirror (NALM), and then show how such a switch can be used within a laser cavity to act as a passive mode-locker. We will then detail the results of experiments on a passive, self-starting, fibre laser capable of generating solitons with durations as short as 320 fs.

A number of all-fibre switching schemes have been developed based on third-order, nonlinear phenomena (i.e., the small change of refractive-index that occurs with optical intensity). All of these schemes require some form of dual-path interferometer (or polarimeter) in order to detect the small phase change that is induced by the third-order nonlinearity. The power levels required to obtain maximum switching contrast in any interferometric switching scheme are determined by the precise design and details of the system but can be roughly estimated from

$$IL = 500$$

where I is the optical power in Watts and L is the interaction length in metres. It can be seen that either high power levels or long interaction lengths are required to get appreciable switching effects. In order to obtain switching powers commensurate with any practical communications or signal-processing system (i.e., < 1 W), we require switches with correspondingly long interaction lengths ($L > 500$ m). Such long interaction lengths lead to severe problems with environmental stability for any interferometric device owing to the difficulty of maintaining a long-term phase balance between the optical paths involved. However, if we adopt a scheme based on the fibre Sagnac interferometer (Fig. 19) in which the two "arms" of the interferometer are common to the same piece of fibre, the system will be inherently stable to perturbations provided that they occur on a time scale that is long compared to the time taken for light to travel through the interferometer, typically a few microseconds. Since the Sagnac interferometer when operating linearly returns light to the port from which it came, it is frequently referred to as a "loop mirror" [39].

A recent development is to incorporate an EDFA within the loop mirror [40, 41] as shown in the figure. Since the amplifier is located at one end of the loop, the counterclockwise propagating light traverses the loop at lower intensity than the clockwise propagating light, and the amplifier provides the necessary switching asymmetry.

The nonlinear response to the system can be obtained by evaluating the response of the coupler (which has equal power-splitting) to light incident at the input port (optical intensity I_1). Considering quasi-CW operation (i.e., a regime in which dispersive effects can be neglected), and assuming an amplifier gain G with an effective-path length L, the net phase difference $\Delta\phi$ between counterpropagating pulses is

$$\Delta\phi = (G - 1)n_2 I_1 kL$$

where k is the propagation vector and n_2 is the nonlinear refractive-index ($n = n_0 + n_2 I_1$). This net phase difference generated after propagation around the loop causes switching of the light from the input to the output ports according to

$$I_2 = GI_1 \sin^2(\Delta\phi)$$

and gives 100% of the input light switched to the outport port at $\Delta\phi = (2n + 1)\pi$, $n = 0, 1, 2, \ldots$. Effectively, the loop mirror reflection *decreases* with input intensity. The high gain available with erbium-doped fibre amplifiers ($G > 40$ dB) reduces input switching powers of fibre switches from the Watt to the microwatt regime. Note that the NALM has inherent gain, which has potential for use as a mode-locking element within a laser cavity.

We have assumed here that the light remains in a linear state of polarization throughout its traversal of the interferometer. This is unlikely to be the case, and the NALM

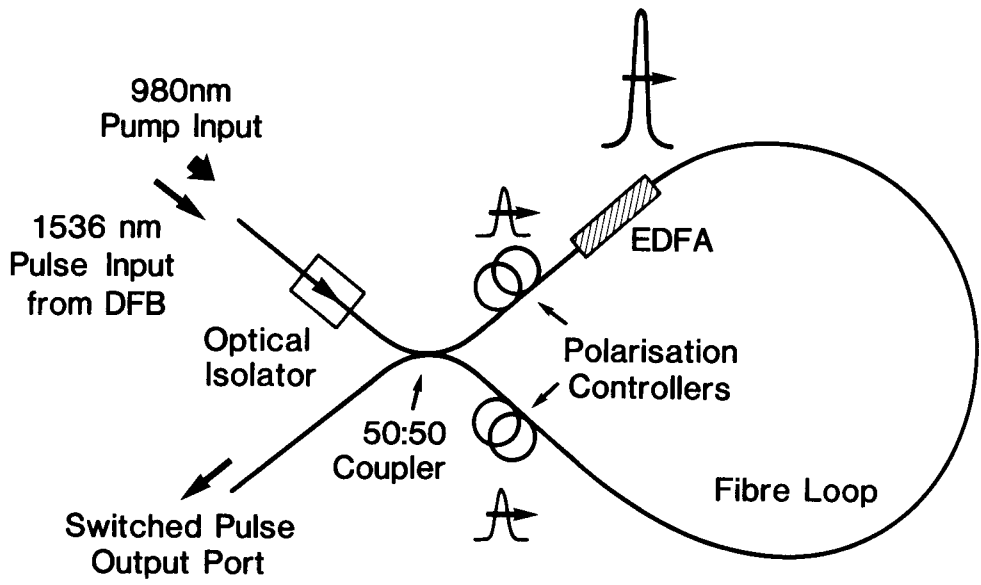

Figure 19. Fibre Nonlinear Amplifying Loop Mirror switch configuration.

loop is almost certain to possess a degree of birefringence. It can be shown that the net effect is to add a linear-phase-bias to the nonlinear phase shift. By appropriate birefringence control (corresponding to an equivalent linear phase shift of π) the NALM switching characteristic can be completely reversed, i.e., the loop-mirror reflectivity can be made to *increase* with intensity, in which form it can be useful as a nonlinear feedback element for a mode-locked laser.

The input/output power transfer characteristic for a high gain (46 dB) NALM is shown in Fig. 20. The loop length was 306 m, the input signal source was a DFB laser

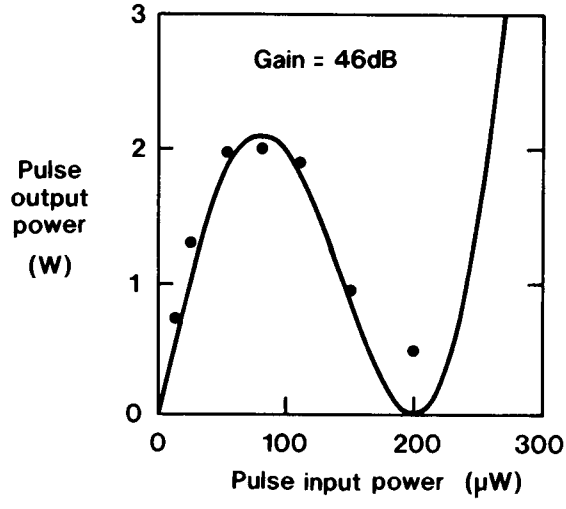

Figure 20. Transfer characteristic of the NALM fibre switch.

operating at a wavelength of 1536 nm. The interferometric nature of the switch is evident from the sinusoidal characteristic. Note that full switching occurs at an input of only 100 μW peak power.

Since the degree of NALM switching is power-dependent and has a transfer function given above, passing a pulse with a given intensity profile through the device leads to strong pulse-shaping effects. It transpires that the only pulses that do not suffer shaping and losses on switching are solitons, since they are the only pulse form (with the exception of square pulses) that have an overall phase factor that applies equally across the entire pulse envelope. It is this unusual attribute that permits low-energy-loss soliton switching in the NALM. This further lends credence to the statement that solitons are the natural bits for communications and switching. The operation of the NALM in the soliton regime has been analyzed for a relatively low-gain system (of the order 3 dB) in [42], where it is concluded that solitons should be well switched by the NALM.

Mode-Locked Fibre Lasers

It is well known from bulk laser theory that the incorporation of nonlinear elements, such as saturable absorbers, within a laser cavity can lead to passive mode-locking of the system and generally yields very short pulses. Provided it is biased using birefringence, the NALM characteristic on the first switching cycle is similar to that of a saturable absorber, only in this case the NALM acts as a mirror whose reflectivity increases with intensity. Such a nonlinear mirror can be used as one end mirror in a Fabry-Perot cavity [43] to produce mode-locking. However, the birefringence control required to bias the NALM leads to environmental instability. A more complex scheme, known as the Figure-8 laser [44–46] does not require birefringence bias of the NALM and is therefore potentially more stable.

The Figure-8 laser scheme is shown in Fig. 21. The system consists of two discrete loops—one a unidirectional ring containing an isolator and the other a NALM loop. At low intensity, light incident at port *A* is reflected back to port *A* by the loop mirror and is therefore ultimately lost within the isolator. However, if the light intensity is high, as might occur for mode-locked pulses, the NALM switches light to port *B*, whereupon it is able to circulate within the isolator loop, providing feedback for the laser.

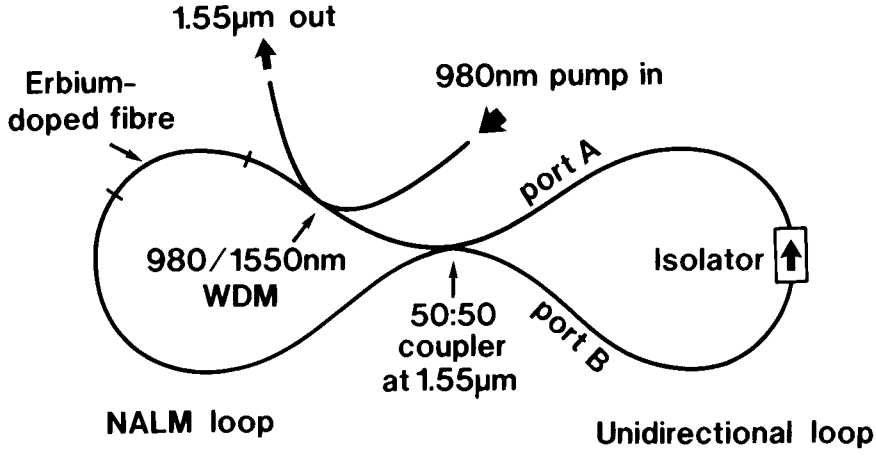

Figure 21. Figure-8 self-starting, mode-locked fibre-laser scheme.

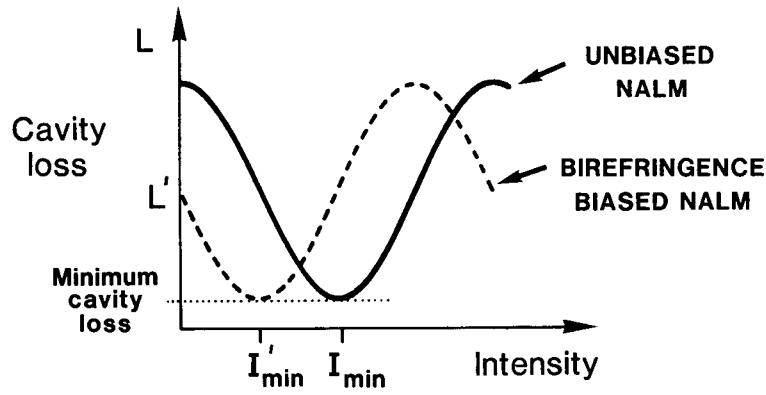

Figure 22. Resonator loss in the Figure-8 laser as a function of intra-cavity (pulse) intensity, showing how the loss can be adjusted by means of birefringence.

If we consider light propagation in the quasi-CW regime, then the cavity loss versus light intensity has the form shown in Fig. 22, where it is seen that there is a well-defined intensity that produces minimum laser resonator loss.

Since the laser system is predisposed to operate in a mode that minimizes internal losses, it favors high-intensity, pulsed operation, i.e., mode-locking. As we saw above, the NALM loop switches with minimum loss pulse waveforms that are either square or solitons, since both of these waveforms have the characteristic that they generate uniform nonlinear phase profiles across their entire pulse envelope. We would therefore expect the laser to favor these pulse forms. Furthermore, the low input powers required to switch a NALM operating at high gain enables the pulsed operation to build up from noise at the NALM input. The process is assisted by allowing a degree of CW lasing at low input pump powers, either by using a coupler with an asymmetric coupling ratio or by biasing the NALM by means of birefringence, as in Fig. 22. Thus the laser operates in pulsed mode without the need for any external modulator and is found to undergo a variety of different types of pulse behavior [47]. Both square pulse and soliton pulse generation have been observed with the system operating at 1.56 μm. The square pulses are relatively long in duration (150 psec).

The more interesting soliton regime can be entered by adjusting the NALM phase-bias (Fig. 22), and the resulting solitons can have a duration as short as 320 fsec. The autocorrelation trace and optical spectrum obtained in this case are shown in Fig. 23. Note the large blue-shifted component of the spectrum, the origin of which is believed to be due to splitting of the pulse into soliton and nonsoliton components during the amplification and propagation processes. These components separate both temporally and spectrally, since the soliton pulse will be red-shifted by the soliton self-frequency shift. The dynamic balance between the self-frequency shift and the gain-pulling effect of the amplifier push the pulse out to the long-wavelength edge of the erbium gain-spectrum. The large blue-shift component is not observed when generating solitons with durations $> \sim 600$ fsec.

Because the laser operates without external modulation, the soliton repetition rate can be complex. Bunches of solitons repeating at the cavity round-trip frequency have been observed, with pulse repetition rates as high as 100 GHz within the pulse bunches. The system can also operate in a regime in which the solitons are no longer bunched but

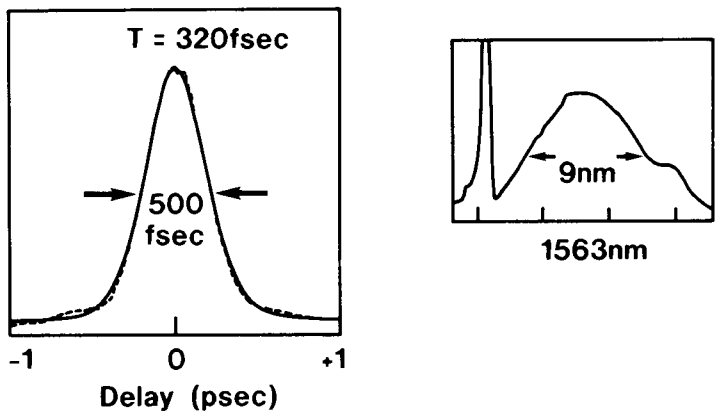

Figure 23. Autocorrelation trace and spectrum of a 320 fs soliton pulse obtained at the output of the Figure-8 laser. Solid line represents the calculated soliton profile.

occur seemingly randomly distributed over the entire cavity round-trip period, the pulse patterns repeating at the round-trip frequency. Note that since the energy of a soliton is fixed, i.e., quantized, more pulses must circulate in the cavity if the pump power is increased. Thus the average repetition rate must increase in order to obtain more output power. It is also possible to obtain pure harmonic mode-locking in which an integral number of precisely spaced pulses occur within a round-trip period.

Despite the very broad gain-bandwidth of erbium ions in silica, the effect of soliton self-frequency shift restricts the minimum possible pulse duration to around 300 fsec, as noted above. By combining the Figure-8 laser and the EDFA, it is possible to generate even shorter pulses by exploiting the pulse compression that occurs during soliton amplification in a fibre amplifier [48]. In this case the Figure-8 laser was configured to produce stably bandwidth-limited soliton pulses with a duration of 450 fsec, using just 20 mW of launched pump power at 980 nm, a power easily obtainable from a laser diode. The average output power was 120 μW with approximately 10 pulses circulating within the laser cavity. The pulses were fed to an external EDFA with a length of 5.5 m. Since a small amount of power was tapped from the full-power solitons circulating within the Figure-8 laser, the input to the amplifier fibre was only about one tenth the peak power required for a soliton. Thus over the first few metres of the amplifier the pulses increase their energy without experiencing significant nonlinear effects. However, when the pulse under amplification attains an energy close to that of the fundamental soliton, nonlinear effects in its propagation become significant and the amplification process becomes more complicated. At a certain pulse energy corresponding to a higher-order soliton, multisoliton compression occurs and the pulsewidth decreases abruptly. With a pump power of 320 mW in the following EDFA, a total power gain of 29 dB was obtained and pulse compression down to 90 fsec was observed at the fibre output. The time-bandwidth product of these pulses was 0.3, in reasonable agreement with that expected for a sech^2 soliton pulse shape. Thus, during soliton amplification and propagation we are able to transform 450 fsec fundamental solitons into 90 fsec fundamental solitons.

A number of interesting further effects could be observed at higher EDFA gains, such as high-order soliton break-up into coloured solitons due to soliton self-frequency

shift [48]. These experiments serve to show both how powerful the combination of fibre lasers and amplifiers can be, as well as the ability of the EDFA to support pulses as short as 90 fsec.

Conclusions

We have seen how the simple expedient of incorporating rare-earth ions into optical fibres has produced a whole new active-fibre technology. The most obvious immediate impact of the technology is in fibre amplifiers, which have revolutionized telecommunications systems design, particularly in undersea routes. The fibre amplifier is generally acknowledged as the most significant development in telecommunications in recent years. Its impact will be to hasten the transference of satellite-based telecommunications to optical fibre transmission for international telephone traffic. The full impact of readily available optical amplification has yet to be felt in telecommunications systems architectures, and we expect radical new proposals in the future, particularly involving soliton transmission and dense wavelength-division-multiplexing.

The fibre laser has still to make as great an impact. Although stable, compact, and rugged, its application as a telecommunications source has yet to materialize. A disadvantage is the need for an external modulator, although for high-speed systems this is essential even for diode lasers in order to prevent frequency chirp and the accompanying dispersion. Thus it may be that fibre lasers will find application only in the high-capacity systems of the future where frequency stability is valued and an external modulator is no disadvantage. On the other hand, it is clear that the wide tunability and the variety of emission wavelengths make the fibre laser very attractive for sensing, metrology, and military applications. In addition, the fibre laser is capable of orders of magnitude higher peak-pulse power than the diode laser and is thus well-suited to ranging, OTDR, and nonlinear optics. It should not be forgotten, however, that many of the high power advantages can also be gained by following a gain-switched diode laser with an EDFA, at least for the 1.55 μm spectral region.

A unique attribute of fibre lasers is their ability to produce solitons when mode-locked. It would appear that solitons are the natural bits for both transmission and switching. Since the required soliton pulse form, peak power, and duration are determined by the transmission fibre characteristics, there is a certain logic in generating them within the fibre. We have also shown that combinations of fibre lasers, amplifiers, and components can be used to construct complex fibre circuits, and it is clear that an integrated fibre device technology is emerging. Using this technology, in the future we can expect high-power CW fibre lasers to rival today's miniature, diode-pumped, crystal lasers.

Acknowledgments

I would like to thank all my colleagues at Southampton University, much of whose work is reported here.

References

1. E. Snitzer, "Optical Maser Action of Nd^{3+} in a Barium Crown Glass," *Phys. Rev. Lett.*, vol. **7**, 444, 1961.
2. J. Stone and C. A. Burrus, "Neodymium-Doped Fiber Lasers: Room Temperature cw Operation with an Injection Laser Pump," *Appl. Opt.*, vol. **13**, 1256, 1974.

3. S. B. Poole, D. N. Payne, and M. E. Fermann, ' Fabrication of Low-Loss Optical Fibres Containing Rare-Earth Ions," *Electron. Lett.*, vol. **21**, 737, 1985.
4. R. J. Mears, L. Reekie, S. B. Poole, and D. N. Payne, "Neodymium-Doped Silica Single-Mode Fibre Lasers," *Electron. Lett.*, vol. **21**, 738, 1985.
5. R. J. Mears, L. Reekie, I. M. Jauncey, and D. N. Payne, "High-Gain, Rare-Earth-Doped Fibre Amplifier at 1.54 μm," *Proc. OFC 1987*, Reno, Paper W12, February 1987.
6. M. Horiguchi, M. Shimizu, M. Yamada, K. Yoshino, and M. Hanafusa, *Electron. Lett.*, vol. **26**, 1733–1759, 1990.
7. M. Shimizu, M. Yamada, M. Horiguchi, T. Takeshita, and M. Okayasu, *Electron. Lett.*, vol. **26**, 1641–1643, 1990.
8. M. Nakazawa, Y. Kimura, and K. Suzuki, Proc. Topical Mtg on Optical Amplifiers & Their Applications, Paper PDP1, Monterey, 1990.
9. M. N. Zervas, R. I. Laming, and D. N. Payne, "Trade-Off Between Gain Efficiency and Noise Figure in an Optimised Fibre Amplifier," *Proc. OFC '92*, San Jose, February 1992.
10. A. H. Gnauck and C. R. Giles, "2.5 Gb/s and 10 Gb/s Transmission Experiments Using a 137 Photon/Bit Erbium Fibre Preamplifier Receiver," *Proc. 17th European Conf. on Optical Commun.* vol. **3**, 60–63, 1991.
11. R. I. Laming, L. Reekie, P. R. Morkel, and D. N. Payne, "Multichannel Crosstalk and Pump Noise Characterisation of Er^{3+}-Doped Fibre Amplifier Pumped at 980 nm," *Electron. Lett.*, vol. **25**, 455–456, 1989.
12. R. I. Laming, D. N. Payne, F. Meli, G. Grasso, and E. J. Tarbox, "Highly-Saturated Erbium-Doped-Fibre Power Amplifiers," *Proc. Topical Meeting on Optical Fibre Amplifiers and Their Appl.*, vol. **13**, 16–19, Monterey, CA, August 1990.
13. S. P. Craig-Ryan, J. F. Massicott, M. Wilson, B. J. Ainslie, and R. Wyatt, *Proc. ECOC '90*, Amsterdam, 1990.
14. H. Takenaka, H. Okuno, M, Fujita, Y. Odagiri, Y. Sunohara, and I. Mito, "Compact Size and High Output Power Er-Doped Fiber Amplifier Modules Pumped with 1.48 μm MQW LDs", *Proc. Second Topical Meeting on Optical Amplifiers and Their Appl.*, vol. **13**, 254–257, Snowmass, Colorado, June 1991.
15. S. G. Grubb, T. H. Windhorn, W. F. Humer, K. L. Sweeney, P. A. Lelabady, J. E. Townsend, K. P. Jedrzejewski, and W. L. Barnes, " +20 dBm Erbium Power Amplifier Pumped by a Diode-Pumped Nd:YAG Laser," *Proc. Second Topical Meeting on Optical Amplifiers and Their Appl.*, Paper PDP 2-1, Snowmass, Colorado, June 1991.
16. J. D. Minelly, R. I. Laming, J. E. Townsend, W. L. Barnes, E. R. Taylor, K. P. Jedrzejewski, and D. N. Payne, "High-Gain Fibre Power Amplifier Tandem-Pumped by a 3W Multistripe Diode," *Proc. OFC '92*, San Jose, February 1992.
17. J. E. Townsend, W. L. Barnes, K. P. Jedrzejewski, and S. G. Grubb, "Yb^{3+}-Sensitised Er^{3+}-Doped Optical Fibre in Silica Host with Very High Transfer Efficiency," *Electron. Lett.*, vol. **27**, 1958–1959, 1991.
18. M. Tachibana, R. I. Laming, P. R. Morkel, and D. N. Payne, "Erbium-Doped Fibre Amplifier with Flattened Gain Spectrum," *Photonics Technology Lett.*, vol. **3**, 118–120, 1991.
19. Y. Miyajima et al., "Nd^{3+}-Doped Fluoride Fiber Amplifier Module with 10 dB Gain and High Pump Efficiency," *Proc. Second Topical Meeting on Optical Amplifiers and Their Appl.*, Snowmass, Colorado, June 1991.
20. Y. Ohishi et al., "Pr^{3+}-Doped Optical Fiber Amplifier Operating at 1.3 μm," *Proc. Optical Fibre Commun. Conf.*, San Diego, 1991.
21. Y. Miyajima et al., "38.2 dB Amplification at 1.31 μm and Possibility of 0.9 μm Pumping in Pr^{3+}-Doped Fluoride Fiber," *Electron. Lett.*, vol. **27**, 1706–1701, 1991.
22. M. Nakazawa, E. Yamada, H. Kubota, and K. Suzuki, "10 Gbit/s Soliton Data Transmission over One Million Kilometres," *Electron. Lett.* vol. **27**, 1270, 1991.
23. W. L. Barnes, P. R. Morkel, L. Reekie, and D. N. Payne, "High Quantum Efficiency Er^{3+} Fibre Lasers Pumped at 980 nm," *Opt. Lett.*, vol. **14**, 1002–1004, 1989.

24. P. Urquhart, "Review of Rare-Earth-Doped Fibre Lasers and Amplifiers," *IEEE Proc. Part J.*, vol. **135**, 385, 1988.
25. W. L. Barnes and J. E. Townsend, "Highly Tunable and Efficient Diode Pumped Operation of Tm^{3+}-Doped Fibre Lasers," *Electron. Lett.*, vol. **26**, 747–756, 1990.
26. E. Snitzer, H. Po, F. Hakimi, R. Tumminelli, and B. C. McCollum, "Double-Clad, Offset Core Nd Fibre Laser," *Proc. Conf. on Optical Fibre Commun.*, New Orleans, Paper PD5, 1988.
27. H. Po, E. Snitzer, R. Tumminelli, L. Zenteno, F. Hakimi, N. M. Cho, and T. Haw, "Doubly Clad High Brightness Nd Fibre Laser Pumped by GaAlAs Phased Array," *Proc. Conf. on Optical Fibre Commun.*, Houston, 1989.
28. J. D. Minelly, E. R. Taylor, K. P. Jedrzejewski, J. Wang, and D. N. Payne, "Laser-Diode-Pumped Neodymium-Doped Fibre Laser with Output Power in Excess of 1 Watt," *Proc. Conf. on Lasers and Electro-Optics*, Paper CWE6, Anaheim, May 1992, (to appear).
29. J. D. Minelly, R. I. Laming, J. E. Townsend, W. L. Barnes, E. R. Taylor, K. P. Jedrzejewski, and D. N. Payne, "High-Gain Power Amplifier Tandem-Pumped by a 3W Multistripe Diode," *Proc. Conf. on Optical Fibre Commun.*, Paper TuG2, San Jose, 1992.
30. I. M. Jauncey, L. Reekie, J. E. Townsend, D. N. Payne, and C. J. Rowe, *Electron. Lett.*, vol. **24**, 24–26, 1988.
31. P. R. Morkel, G. J. Cowle, and D. N. Payne, *Electron. Lett.*, vol. **26**, 632–634, 1990.
32. W. V. Sorin and H. J. Shaw, *J. Lightwave Technology*, vol. **LT-3**, 1041–1043, 1985.
33. G. Meltz, W. W. Morey, and W. H. Glenn, *Optics Lett.*, vol. **14**, 823–825, 1989.
34. J. Stone and D. Marcuse, *J. Lightwave Technology*, vol. **LT-1**, 382–385, 1986.
35. I. Bennion, D. C. J. Reid, C. J. Rowe, and W. J. Stewart, *Electron. Lett.*, vol. **22**, 341, 1986.
36. W. W. Morey, *Proc. OFS '90*, 285, Sydney, Australia, 1990.
37. J. Stone and L. W. Stulz, *Electron. Lett.*, vol. **23**, 781–782, 1987.
38. See, for example, P. W. France (Ed.), "*Optical Fibre Lasers and Amplifiers*," Chapter 9, Blackie & Son, London, 1991, ISBN 0-216-93157-6.
39. N. J. Doran, K. J. Blow, and D. Wood, "Soliton Logic Elements for All-Optical Processing," *SPIE*, vol. **836**, Optoelectronics Materials, Devices, Packaging, and Interconnects, 238–243, 1987.
40. D. J. Richardson, R. I. Laming, and D. N. Payne, "Very Low Threshold Sagnac Switch Incorporating an Erbium Doped Fibre Amplifier," *Electron. Lett.*, vol. **26**, 1779, 1990.
41. A. W. O'Neill and R. P. Webb, "All Optical Loop Mirror Switch Employing an Asymmetric Amplifier/Attenuator Combination," *Electron. Lett.*, vol. **26**, 2008–2009, 1990.
42. M. E. Fermann et al., "Nonlinear Amplifying Loop Mirror," *Optics Lett.*, vol. **15**, 1217–1224, 1990.
43. H. E. Avromopolous et al., "A Passively Mode-Locked Erbium Fibre Laser," *Topical Meeting on Optical Amplifiers & Their Applications*, Monterey, Paper PDP8, 1990.
44. D. J. Richardson et al., "Self-Starting Passively Mode-Locked Fibre Laser Based on the Amplifying Sagnac Switch," *Electron. Lett.*, vol. **27**, 542, 1991.
45. I. N. Duling, III, "All-Fiber Ring Soliton Laser Model-Locked with a Nonlinear Mirror," *Optics Lett.* vol. **16**, 539–541, 1991.
46. A. G. Bulshev, E. M. Dianov, and O. G. Okhotinov, "Self-Starting Mode-Locked Laser with a Nonlinear Ring Resonator," *Optics Lett.*, vol. **16**, 88–90, 1991.
47. D. J. Richardson et al., "Pulse Repetition Rate Effects in a Passively Mode-Locked Erbium Doped Fibre Laser," *Electron. Lett.*, vol. **27**, 1451–1453, 1991.
48. D. J. Richardson, A. B. Grudinin, and D. N. Payne, "Passive, All-Fibre Source of 30 fs Solitons," *Proc. Topical Meeting on Non-Linear Guided Wave Phenomena*, Paper PDP8, Cambridge, September 1991.